frontiers | Frontiers in Astronomy and Space Sciences

TYPE Brief Research Report
PUBLISHED 08 August 2022
DOI 10.3389/fspas.2022.919828

OPEN ACCESS

EDITED BY
Chandra Sivaram,
Indian Institute of Astrophysics, India

REVIEWED BY
Brandi L. Carrier,
NASA Jet Propulsion Laboratory (JPL), United States
Fulvio Franchi,
Botswana International University of Science and Technology, Botswana

*CORRESPONDENCE
S. S. Johnson,
sj599@georgetown.edu

SPECIALTY SECTION
This article was submitted to Astrobiology, a section of the journal Frontiers in Astronomy and Space Sciences

RECEIVED 14 April 2022
ACCEPTED 05 July 2022
PUBLISHED 08 August 2022

CITATION
Roussel A, McAdam AC, Graham HV, Pavlov AA, Achilles CN, Knudson CA, Steele A, Foustoukos DI and Johnson SS (2022), Diagnostic biosignature transformation under simulated martian radiation in organic-rich sedimentary rocks.
Front. Astron. Space Sci. 9:919828.
doi: 10.3389/fspas.2022.919828

Diagnostic biosignature transformation under simulated martian radiation in organic-rich sedimentary rocks

A. Roussel [1], A. C. McAdam [2], H. V. Graham [2], A. A. Pavlov [2], C. N. Achilles [2,3,4], C. A. Knudson [2,3,4], A. Steele [5], D. I. Foustoukos [5] and S. S. Johnson [1,6]*

[1]Department of Biology, Georgetown University, Washington, DC, United States, [2]NASA Goddard Space Flight Center, Greenbelt, MD, United States, [3]Center for Research and Exploration in Space Science and Technology, Greenbelt, MD, United States, [4]Department of Astronomy, University of Maryland, College Park, MD, United States, [5]Earth and Planets Laboratory, Carnegie Institution for Science, Washington, DC, United States, [6]Science, Technology, and International Affairs Program, Georgetown University, Washington, DC, United States

As we look for traces of ancient life on Mars, we need to consider the impact of ionizing radiation in the biosignature preservation process. Here, we irradiated two organic rich terrestrial samples (Enspel and Messel shales) that have Martian analog mineralogies, with simulated cosmic rays to a dose of 0.9 MGy, equivalent of 15 million years of radiation exposure on the Martian surface. We compared a range of biosignatures before and after exposure, including total organic carbon, bulk stable carbon isotope ratios, diagnostic lipid biomarkers (hopanes and steranes), and Raman signatures akin to those collected by the Scanning Habitable Environments with Raman and Luminescence for Organics and Chemicals (SHERLOC) instrument on Perseverance. While we did not observe a significant difference in total organic carbon, bulk stable carbon isotopes, or Raman G-band signatures, we found that five lipid biomarkers decreased by a factor of two to three in the Enspel shale. This degree of degradation exceeds current predictions by existing models or experimental studies in organic rich samples and challenges our current understanding of complex biosignatures under ionizing irradiation.

KEYWORDS

cosmic rays, biosignatures, Mars, analogs, irradiation

Introduction

After decades of research and several robotic spacecraft, we know today that Mars was habitable early in its history (Squyres and Kasting, 1994; Grotzinger et al., 2014). But 3.7 to 4.1 billion years ago, the red planet lost its magnetic field (Acuna et al., 1999; Mittelholz et al., 2020). Without a protective magnetic field and with a thin atmosphere, solar radiation and energetic particles were able to reach the surface, and the Martian surface progressively turned into a freezing irradiated desert. However, there was a small window of surface habitability, and an important challenge is to discover whether life evolved in

that period of time and furthermore, if any trace of this evolution remains that we could detect today.

To answer these questions, several robotic rovers have been sent to the Mars, including NASA's *Curiosity* and *Perseverance* rover missions, which arrived in 2012 and 2021, and in the future, ESA's *Rosalind Franklin* rover mission will join them. Detecting biosignatures, or traces of ancient life, is one of the main objectives of *Perseverance* and *Rosalind Franklin* (Vago et al., 2015; Farley et al., 2020). To target the best preserving environments for ancient biosignatures, it is crucial to understand the forces and processes that may affect the preservation potential of biosignatures (in particular organic biomarkers) and the capability of rover-based instrumentation to detect them. As such, radiation effects that degrade organic molecules at the planet's surface are key to understanding biosignature preservation and will serve to enable targeting the environments that best preserve possible ancient biosignatures on Mars.

Much of our understanding of biosignature degradation on the planet's surface derives from using the Earth as an analog. Biosignature taphonomy on earth has been extensively studied (e.g., Eigenbrode, 2008; Summons et al., 2008), but an additional challenge to the persistence of ancient biosignatures in the Martian environment exists: For billions of years, the Martian surface has been exposed to high-energy radiation. The most abundant source of radiation on Mars is Solar Energetic Particles (SEPs), absorbed in the first few centimeters of the surface. SEPs can measure up to 10^8 eV, and are composed of protons, electrons, and heavier nuclei (Horneck and Baumstark-Khan, 2002). Galactic Cosmic Rays (GCRs), however, are more powerful; they range to over 10^{21} eV (Simpson, 1983) and can penetrate several meters into the subsurface (Dartnell et al., 2007). GCRs are produced outside the Solar System and composed primarily of protons and alpha particles, as well as some high-energy nuclei. Reacting with the planet's atmosphere and regolith, GCRs produce secondary particles (neutrons, pions, positrons, muons) that rapidly decay into mostly gamma rays (Dartnell et al., 2007). For this reason, gamma rays serve as a suitable analog for GCR exposure in the top few centimeters to meters into the Martian subsurface.

Current technology allows drilling to relatively shallow depths on Mars: 5 cm for *Curiosity* (Okon, 2010), 7.6 cm for *Perseverance* (Moeller et al., 2021), and up to 2 m for the developed *Rosalind Franklin* rover (Vago et al., 2015). While *Rosalind Franklin* will uncover samples that have been more shielded from GCRs than *Curiosity* and *Perseverance*, cosmic rays may still impact the preservation of organic biosignatures recovered at the depth this mission will drill. So far, no direct evidence of biomolecules that are unambiguously diagnostic of life have been detected at the Martian surface. While simple abiogenic organics can survive across geological time on Mars (Steele et al., 2012; Freissinet et al., 2015; Glavin et al., 2015; Eigenbrode et al., 2018; Steele et al., 2018; Freissinet et al., 2020; Steele et al., 2022), it remains to be seen whether complex organic molecules near the surface of the planet have a similar robustness. Farley et al. (2014) showed that even if the sedimentary rocks in Gale crater were deposited when the planet was habitable, 4.21 ± 0.35 billion years ago (Sheepbed mudstone at Yellowknife Bay), they have likely been exposed to cosmic rays for a much shorter time: 78 ± 30 million years (Myr). A later study (Martin et al., 2017) estimated that another sample in Gale crater (Mojave 2) was exposed for a significantly longer time, 300 Myr to 1 Gyr (billion years). These measurements give us crucial insight into how much the surface was exposed to radiation over time. However, they are not representative of the whole planet; as some facies, such as those recently exposed by wind-blown scarp retreat may have even shorter exposure times, while other facies could have been exposed for several billion years. To help guide sample selection, it is critically important to understand how diagnostic biosignatures are degraded by GCRs across representative geological timelines. This is particularly important when considering the goals of Mars Sample Return, which will enable the scientific community to study a limited but important subset of Martian rocks and soils using sophisticated laboratory instruments.

The goal of this study was to analyze the diagenesis of diagnostic organic biosignatures in naturally occurring Mars analog samples under a controlled cosmic ray exposure regimen. We focused on GCRs, the dominant deleterious form of radiation at the depths accessible to the rovers utilizing current drilling and sampling instrumentation (Pavlov et al., 2012). As gamma rays are major degradation particles from GCRs, we used gamma rays as a GCR analog. This study focuses on three classic types of biosignature analyses: chemical and isotopic analyses, as well as spectral characterization.

We focused on two primary samples for this study: the Enspel (~23–28 Myr) and the Messel (~47 Myr) shale (Robinson et al., 1989; Lüniger and Schwark, 2002). The shales are natural lithified muds which contain significant smectite clay minerals while also importantly containing the naturally preserved lipid biomarkers that are the focus of this work. Smectite clay minerals have also been found in significant abundances (up to ~34 wt. %) in fine-grained lacustrine/fluvial Martian sedimentary rocks such as the Sheepbed mudstone (e.g., Vaniman et al., 2014) and several sedimentary rocks in the Glen Torridon clay-bearing unit (Bristow et al., 2021; Thorpe et al., 2021) investigated by the Curiosity rover. Additionally, smectite clay minerals and other phyllosilicates have been detected on Mars both orbitally (Poulet et al., 2005; Ehlmann et al., 2011; Fraeman et al., 2016) and *in situ* in Gale crater (e.g., Rampe et al., 2020). X-Ray Diffraction (XRD) analyses of our samples indicate that the Enspel Shale consists of the smectite clay mineral montmorillonite, as well as illite, kaolinite, plagioclase and quartz and the Messel Shale consists of montmorillonite, trace

kaolinite, siderite, and quartz. The samples were both dominated by smectite clay minerals. Clay minerals are preferred targets for astrobiology (McMahon et al., 2018), and especially for Mars Sample Return as they are a favorable environment for the preservation of high concentrations of diverse biosignatures over geological timescales (Summons et al., 2011).

The gamma ray radiation exposure utilized in this study (0.9 MGy, mega gray) is equivalent to 15 Myr of radiation exposure at the Martian surface according to the model of Pavlov et al. (2012). Though there are subtle differences between artificial and natural irradiation such as the rate of received dose, and potentially kinetic alterations and/or reactivity levels, this method is commonly used to mimic GCRs (Kminek and Bada 2006; Rojas Vivas et al., 2021; Pavlov et al., 2022).

We then compared three types of organic biosignatures in our control samples and irradiated samples. Initially, we focused on total organic carbon (TOC) and bulk stable carbon isotope ratios. The TOC quantifies the organic content of the sample, and the bulk stable carbon isotope ratio provides information about potential biotic sources of carbon (Peters et al., 2005): as ^{12}C is assimilated faster than ^{13}C by enzymes, biotic carbon tends to have a higher ^{12}C content, so a lower $^{13}C/^{12}C$ ratio value. We hypothesize that the general destruction of organic matter into volatile CO_2 or CH_4 would lead to a decrease of TOC after irradiation. Even though gamma rays are not isotopically selective in their interactions, we analyzed the samples to determine if secondary oxidants could shift the isotopic ratio.

The chemical biosignatures we targeted are diagnostic lipid biomarkers in the form of hopanes and steranes: some of the most persistent components of cell membranes, and are specific to and therefore diagnostic for prokaryotic and eukaryotic life respectively (Brocks and Summons, 2003). While it may appear unlikely to find such complex terrestrial molecular fossils on the Martian surface, we use them here as a best-case scenario as one of the most persistent diagnostic traces of terrestrial life, as a terrestrial biochemistry-based analog for recalcitrant molecules that perform a similar function within any putative Martian organism. They are molecular fossils of the biochemical precursor molecules hopanols and sterols (Eigenbrode, 2008). During diagenesis, hopanols and sterols lose their functional groups, whereas their diagnostic hydrocarbon skeleton can be preserved over the geological timescale (Brocks and Summons, 2003). This hydrocarbon structure, if found on another planet, is peculiar enough to be diagnostic of life, as there is no known abiotic synthesis pathway. Our interest here was not to identify the biotic sources of biomarkers (that has been well described in the literature (Robinson et al., 1989; Lüniger and Schwark, 2002)), but to investigate how complex molecular signatures change under cosmic ray exposure using these molecules as a terrestrial analog to complex compounds in a putative Martian organism.

The Enspel and Messel samples were also analyzed using Raman spectroscopy, specifically targeting the spectral signature of the diagnostic G-band (its position and width). It is known that factors such as sample maturity, thermal degradation, starting composition, possible graphite domain size, lead to a shift in the characteristic D (~1,350 cm-1) and G (~1,580–1,600 cm-1) Raman band parameters (Pasteris and Wopenka, 2003). Within this study, we hypothesized that these bands may change in characteristic ways following gamma ray exposure. These analyses also serve as analogs for current flight-like analyses such as the SHERLOC and Supercam instruments aboard the *Perseverance* rover and could help the rover team in selecting samples most likely to contain organic signatures for eventual Earth return from Mars.

Materials and methods

Sample preparation and irradiation

All materials in contact with the samples were solvent cleaned with methanol and dichloromethane (DCM), then heated at 550°C overnight, to prevent laboratory organic contamination. The samples were powdered and sieved (400 μm) to homogenize the indigenous organic matter. We powdered our clay-dominant samples with a gentle non-smearing motion to mitigate against introducing turbostatic disorder. The mortar temperature was regularly checked with a laser thermometer to ensure it did not increase above room temperature.

We used ~1 MeV gamma rays from a ^{60}Co source at a rate of 8.15 Krad (Si)/min to simulate cosmic rays at the NASA Goddard Space Flight Center (GSFC) Radiation Effects Facility (REF). The samples received a total dose of 0.9 MGy with up to 10% variation due to experimental set up. The samples were irradiated in flame-sealed glass vials to avoid contamination from plastic caps. They were sealed under vacuum (~30 mTorr) to remove all air from the tube, as oxygen and water in the air might indeed increase the destruction rate by creating reactive radicals (Dartnell, 2011; Pavlov et al., 2022). Every sample was irradiated in triplicate for extra security in the unlikely event of an accident during exposure, such as tube breaking, and to take into account natural variation of organic material in the samples. Temperature monitoring experiments in the REF have confirmed that our samples stayed under 30°C during irradiation.

XRD

Unirradiated samples were crushed and sieved to <53 μm, and XRD patterns were acquired with a Bruker D8 Discover diffractometer at NASA GSFC from random powder X-ray diffraction analysis mounts, from 2–70°2θ, at 0.01°/step and at least 2 s/step. These patterns enabled the bulk mineralogy of the samples (minerals present and their abundances) to be

determined. To obtain detailed knowledge of the clay mineralogy, oriented mounts of the clay size fraction (<2 μm) were prepared for XRD analysis. Diffraction patterns were acquired for air-dried and glycolated oriented mounts allowing for a thorough assessment of clay mineral 00L peak and discrimination between smectite and illite clay minerals.

Organic extraction, GC-MS, GC-FID and statistical analyses

Solvent-soluble chemical biomarkers were solvent-extracted by a MARS6 microwave digestion system using DCM:Methanol 9:1 for 15 min at 100°C. The solvent-powder mixture was then filtered on an organically clean glass vacuum column using solvent-cleaned 1.1 μm glass filters. The solvent extract was dried down under nitrogen using a Rapidvap evaporator. Potential elemental sulfur was removed from the organic extract by reacting with acid-activated copper overnight. The apolar fraction was obtained by dissolving the dried extract in 10 ml hexane and filtering through an organic clean glass fiber filter to remove any debris or particles. This study focused only on the apolar fraction containing hydrocarbon lipids biomarkers.

Biomarkers were identified with Gas Chromatography—Mass Spectrometry (GC-MS) (Georgetown University) and quantified with Gas Chromatography—Flame Ionization Detector (GC-FID) (MIT) using the same injection standard (deuterated 5-a Cholestane). The samples were injected in splitless mode at 250°C, with Helium as carrier gas. We used a DB-5MS column (60 m × 250 μm × 0.25 μm) in the GC oven, with a temperature held isothermally at 60 °C for 2 min, ramped to 320°C at a rate of 3°C/min, and then held at this temperature for 20 min. The transfer line and source temperatures were respectively set at 300 and 250°C, and the electron energy at 70 eV. GC-MS analyses confirmed that our four types of blanks had none or non-significant contamination: blanks of irradiation, of extraction, of instruments, and of all three previous sources cumulated. Xcalibur and ChemStation were used for, respectively, identification and quantification of biomarkers.

To compare biomarkers concentrations before and after irradiation, we used R to check the hypothesis of normality and equality of variances, and then compared the data with a Student t test. A *p*-value above 0.05 indicated no significant difference in the concentration after irradiation.

EA-IRMS

Organic carbon and bulk stable isotopic composition were determined by combustion in an elemental analyzer (Carlo Erba NC 2500) interfaced through a ConfloIII to a Delta V Plus Isotope Ratio Mass Spectrometer (IRMS) at the Earth and Planets Laboratory at Carnegie (Foustoukos et al., 2021). Prior to the analyses, the samples were treated with 10% HCl solution overnight to remove carbonates and then thoroughly rinsed with millipure water to remove acid residue before being freeze dried overnight. Replicate analyses were performed for each sample. Acetanilide (C_8H_9NO) was analyzed at regular intervals to monitor the accuracy of the measured isotopic ratios and elemental compositions. Uncertainties reported correspond to the 1s deviation between replicates analysis, and they are higher than the precision with respect to standards. For bulk stable carbon isotopes, the internal uncertainty was 0.2 for the first set of replicates and 1.2 for second and third sets of replicates.

Raman spectroscopy

Raman analyses were conducted using a Witec α-300R Scanning Raman spectrometer able to do confocal Raman spectroscopic imaging. To aquire the spectra we used 438 nm excitation laser and two different objective lenses; a ×100 long working distance (LWD) and a ×20 LWD. Light from the sample is fed after collection *via* fibre optic to a f/4 300 mm focal length imaging spectrometer using a 600 lines/mm grating connected to an Andor Peltier-cooled electron multiplying charge-coupled device (EMCCD). Witec Project software was used to remove cosmic rays, undertake background subtraction and to label and deconvolve the G band peak parameters. Typically, small images of areas of the sample in focus were conducted that were 218 × 136 μm in size and containing 25,600 pixels using an integration time of 3 seconds. These data were then screened for the presence of D and G band peaks. At which point these peaks were isolated for G and peak position and full width half max parameter deconvolution. In some cases, single spectra were collected and these typically used a 2 s integration time for 30 s.

Results

After exposing the samples to 0.9 MGy of gamma rays, we found that the TOC, the bulk stable carbon isotope ratio and Raman G-band didn't change significantly (Figure 1, see Supplementary Table S1 for all results). We measured high TOC values around 22 %wt and 30 %wt for Enspel and Messel respectively, an isotope $\delta^{13}C$ value of 27‰ for both samples, and a Raman G band centered between 1,582 cm^{-1} and 1,588 cm^{-1}.

Concerning organic biomarker biosignatures, we identified in both samples five hopanes (29norhop-17 (21)-ene, hop-17 (21)-ene, C_{30} hopane, hop-21 (22)-ene, C_{31} hopane) and two steranes (C_{29} dimethyl cholestane, and C_{31} sterane) with masses ranging from 386 to 428 Da (identified with fractionation patterns on mass spectra, structures in Supplementary Figures S1, S2, masses in Supplementary Table S1). All identified biomarkers were still detectable after irradiation, as seen on

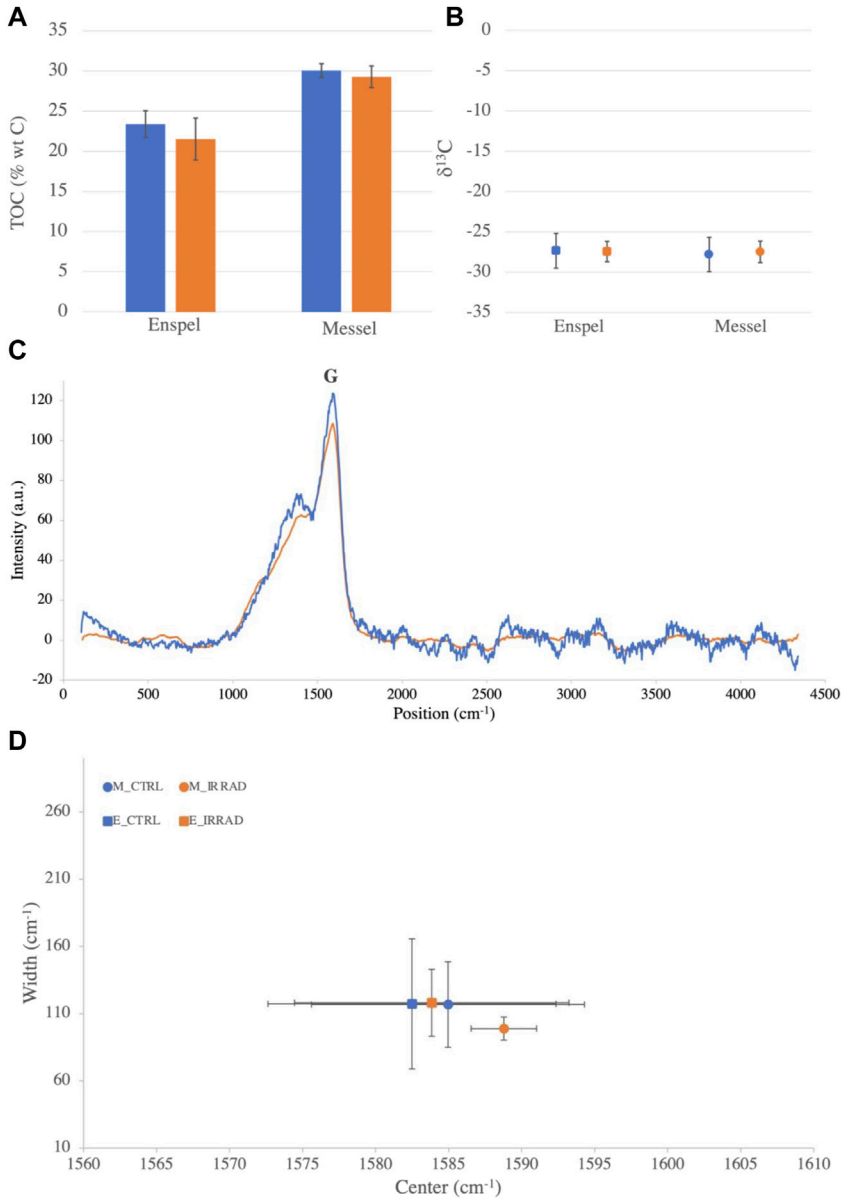

FIGURE 1
Changes of TOC, bulk stable carbon isotopes ratios and Raman G-band. **(A)** Enspel and Messel shales TOC before (blue) and after (orange) an equivalent of 15 Myr of radiation exposure on Mars. **(B)** d^{13}C isotope ratios in Enspel (squares) and in Messel (circles) before (blue) and after (orange) irradiation. **(C)** Raman spectra of Enspel G band before (blue) and after (orange) irradiation. **(D)** Plot of G band parameters (center position vs. width) for Enspel (squares) and Messel (Circles) before (blue) and after (orange) irradiation. Smaller error bars for irradiated Messel shale (orange) are due to a smaller sample size during Raman data acquisition. For all figures, error bars take into account instrumental error and natural variation of organic content in the samples.

the chromatograms of Figure 2. After quantification and statistical comparison of the biomarkers, we didn't observe any significant decrease in the Messel shale (p value > 0.05) (Supplementary Figure S3). In the Enspel shale, however, we observed a significant decrease of all biomarkers (hopanes and steranes) except hop-21-ene and C_{30} hopane by a factor of two to three (Figure 2, lower panel).

Discussion

Generally, we expected a decrease in TOC after a degradation of the organic matter as molecules broke down and degassed as carbon dioxide or methane (Rojas Vivas et al., 2021). In our study, however, the irradiation dose did not appear to be high enough to register significant changes in TOC (Figure 1A). This could be

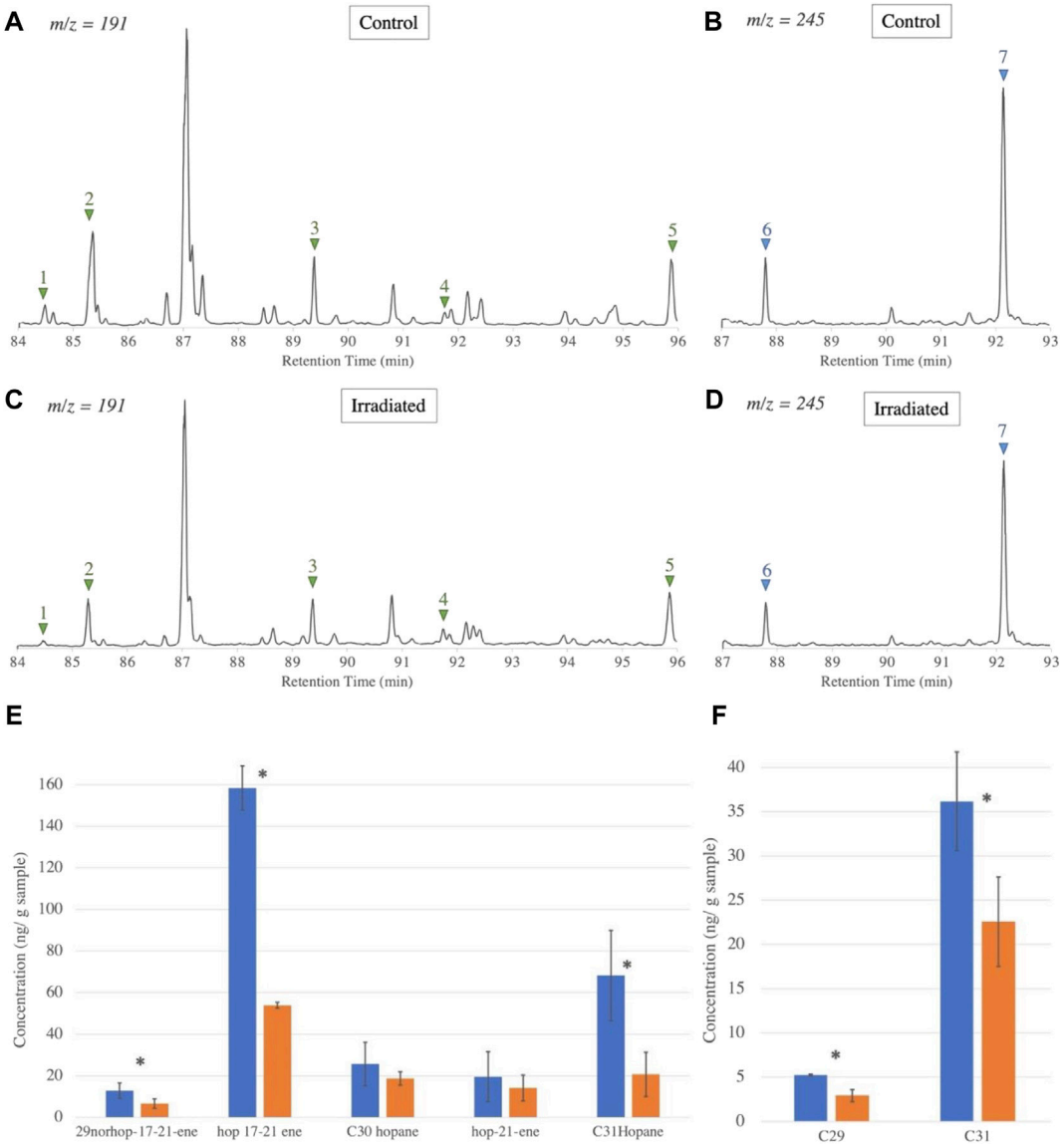

FIGURE 2
Enspel biomarkers chromatogram ion extracts and corresponding concentrations before and after irradiation. Identified hopanes [**(A,C)**, *m/z* = 191)] and methyl-steranes [**(B,D)**, *m/z* = 245)], before **(A,B)** and after **(C,D)** irradiation. Hopanes indicated by a green triangle: (1) 29norhop-17 (21)-ene, (2) hop-17 (21)-ene, (3) C_{30} hopane, (4) hop-21 (22)-ene, (5) C_{31} hopane. Steranes indicated by a blue triangle: (6) dimethyl cholestane (C29), (7) C_{31} sterane. (Structures detailed in Supplementary Figure S1). Concentration of hopanes **(E)** and steranes **(F)** before (blue) and after irradiation (orange). Error bars take into account instrumental error and natural variation of organic content in the samples (irradiated, extracted and measured in triplicates). Concentrations in ng molecule per g of sample. The star shows a significant difference between irradiated and control values (*t* test *p*-value < 0.05).

explained by the significantly higher TOC compared to the natural samples studied by Rojas Vivas et al. (2021). This would indicate that the more organic matter the sample contains, the more reduced conditions prevail, and therefore, a lower production of oxidative radical under ionizing radiation. It should be noted, however, that samples on Mars are known to have lower organic concentrations than those tested here [around 10–12 ppm on Mars and in Martian meteorites (Steele et al., 2016; Eigenbrode et al., 2018)].

For the bulk stable carbon isotope ratios, we didn't expect gamma radiation itself to cause a shift, but induced oxidizing radicals could cause fractionation. The fact that we do not observe any significant change in this ratio either could also be explained by the large concentration of organic matter in our samples (Figure 1B). High organic matter concentration would limit the production of secondary oxidants under radiation, which could further damage the organic matter and fractionate the stable carbon isotope ratio.

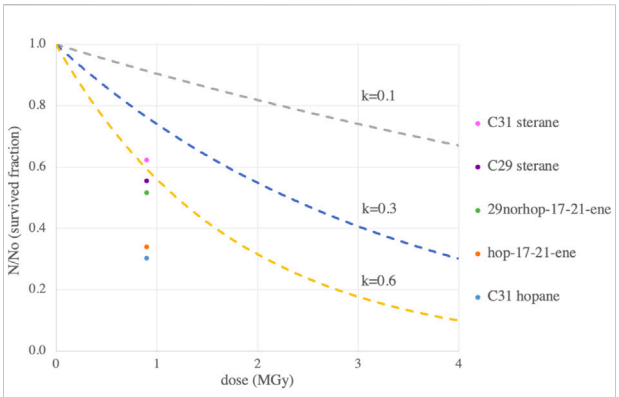

FIGURE 3
Low surviving fraction for most our Enspel biomarkers compared to three other studies. Three radiolysis constants from three studies: k = 0.1 for pure amino acids in Pavlov et al., 2022 (grey), k = 0.3 for low TOC natural samples in Rojas Vivas et al., 2021, and k = 0.6 from Kminek and Bada, 2006 projected to higher masses (428 Da). The significantly decreasing 3 hopanes and 2 steranes survived fractions are represented by dots at our dose of 0.9 MGy.

As the Raman G-band position and width are impacted by initial composition, thermal maturity, and possible graphitic components (Pasteris and Wopenka, 2003), we initially hypothesized that irradiation or the induced oxidative environment would impact the G band parameters. But as mentioned above, the high concentration of organic matter might help limit the amount of induced secondary oxidants, and could explain why the G band parameters were not altered significantly (Figures 1C,D).

Following the same logic, the absence of significant changes in biomarkers concentrations that we measured in the Messel shale was expected. However, the significant decrease of hopane and sterane concentrations in reduced samples (i.e., organic rich) after 0.9 MGy of gamma rays exposure under vacuum is unexpected according to the current models and experimental predictions of organic matter radiolysis. To illustrate this, we compared our results to three other studies (Figure 3).

Organic matter destruction under radiation follows the exponential decay equation:

$$N/No = e^{-k \times D}$$

N/No is the surviving fraction. No is the initial concentration and N the concentration after irradiation. D is the irradiation dose (MGy) and k is the radiolitic constant (MGy^{-1}). The radiolitic constant k is the parameter compared to characterize the rate of the molecule destruction. A study by Rojas Vivas et al. (2021) on low TOC samples measured a value of k = 0.3 MGy^{-1} (blue line on Figure 3). All of the biomarkers studied have a lower survival fraction than they predict, which indicates an overestimation of survivability of these molecules in the Enspel sample used in our study. As the Rojas Vivas et al. (2021) studied radiation effects on low TOC samples, we also compared our results to the k value found by Pavlov et al. (2022), k = 0.1 MGy^{-1}, for pure amino acids, which were closer in TOC to the more to organic-rich samples used in this study (gray line on Figure 3). Once again, our biomarkers (except C30 hopane and hop-21-ene) degraded faster than predicted. However, Pavlov et al. concentrated their study on amino acids, which have a much lower molecular mass than the hopanes and steranes we analyzed. Kminek and Bada (2006) determined a linear correlation between the mass of the molecule and its radiolytic constant. This correlation was also estimated for amino acids with masses ranging from 50 to 150 Da. Extrapolation of this constant to masses in the 300–500 Da range of hopanes and steranes (Supplementary Figure S4), resulted in a k value of k = 0.6 MGy^{-1} for a mass of 428Da, the heaviest compound we analyzed (yellow line on Figure 3). This final prediction, closer in mass to the samples and organics we studied, represented the maximal decrease we should observe according to theory. While most of the biomarkers studied in the Enspel shale are close to the theoretical expected decrease, the hop-17-21-ene and C31 hopanes are much more degraded than expected from these studies with a survived fraction of approximately 30%, a factor of two lower than predicted.

This difference between the experimental results on Enspel shale biomarkers decrease and the three predictions from previous studies may be explained by the use of natural samples in this study instead of synthetic mixes (Kminek and Bada, 2006; Pavlov et al., 2022), which would introduce other confounding factors than previous experiments and models. It could also be representative of larger hydrocarbon biomarkers, compared to previously studied organic molecules such as amino acids. As such this study represents an important observation for the detection of biomarkers for terrestrial life on Mars and as such helps to constrain diagnostic hydrocarbon biomarkers preservation under GCRs.

The studied biomarkers decreased significantly only in the Enspel shale and not in the Messel shale. This difference between our samples could be explained by a different hydration state of the clay minerals: i.e., if the Enspel shale smectite had a higher initial interlayer water content, it could have created more oxidizing radicals under gamma ray exposure, creating a more destructive environment for the biomarkers (Pavlov et al., 2022). This is something we hope to test with future experiments. In addition, mineralogical variation may play a role with some mineralogies becoming more reactive under radiation exposure and creating more oxidative radical damage to co-existing organic material (Ertem et al., 2021). Even though the two samples appear mineralogically very similar, mostly composed of smectite clays, differences in minor mineral components may be leading to more destructive conditions for the analyzed biosignatures. Another possible explanation could be differing initial concentration of organic matter between the two samples (Figure 1), with the Messel shale having ~5%wt more TOC than the Enspel shale. As discussed previously, a higher initial concentration of organic matter makes the sample more reduced and less likely to create oxidative radicals under ionizing radiation (Pavlov et al., 2022).

Conclusion

After analyzing natural samples with Martian analog mineralogies exposed to an equivalent of 15Myr of irradiation on the Martian surface, we found that TOC, carbon isotopes and some molecular biomarkers did not significantly change. This validated some aspects of current models and experimental predictions based on previous studies (Kminek and Bada, 2006; Rojas Vivas et al., 2021; Pavlov et al., 2022), that such organic rich samples should not present any decrease in organic molecule concentrations after 0.9 MGy.

However, in the Enspel shale, most of our chemical biosignatures (29norhop-17-21-ene, hop-17-21-ene, C31 hopane, C29 and C31 sterane) decreased by a factor of 2 to 3 after exposure to gamma rays. This important and unexpected biomarker decrease challenges our estimations of organic matter degradation under ionizing radiation and could be explained by the fact that we studied natural samples, where more parameters can participate in organic destruction than in synthetic mixtures. Additionally, hopanes and steranes biomarkers degradation under gamma rays have never been studied before, and even though we don't expect these exact molecules on Mars, they represent a terrestrial analog of complex and diagnostic chemical biosignatures. This unforeseen biomarker concentration decrease could suggest that such complex biosignatures are even less likely to be preserved on the Martian surface than suggested by the current estimates (Kminek and Bada, 2006; Rojas Vivas et al., 2021; Pavlov et al., 2022), and at the depths where the rover missions are currently looking for traces of ancient life.

These results call for future work to better understand the fate of diagnostic biosignatures under radiation in analog natural samples and to explore the differences highlighted here between the 25 Ma Enspel and 50 Ma Messel samples. A comparison of the transformations that occur under radiation in a diversity of mineralogies could determine if classically targeted parameters (such as smectite-rich samples similar to the shales analyzed in this study) are still relevant targets of high biosignature preservation when exposed to GCRs. In addition, higher irradiation doses would help estimate the exposure time until diagnostic hydrocarbon signatures could be fully erased from the near surface rock record on Mars, as well as defining more precise estimates of the radiolytic constant for a range of biomarkers in natural samples.

Data availability statement

The datasets presented in this study can be found in online repositories. The names of the repository/repositories and accession number(s) can be found below: All reported GC-MS data have been deposited in the FigShare repository at https://figshare.com/s/cc6d2687a57c810f1f64 and GC-FID data at https://figshare.com/s/ca9fd937660c86ddf394. Raman spectra have been deposited in the FigShare repository at https://figshare.com/s/c81cf041e133c79488d7, XRD raw data have been deposited in the FigShare repository at https://figshare.com/s/9ff116fbbf7fb0d900d9, and TOC and bulk stable carbon isotopic data have been deposited in the FigShare repository at https://figshare.com/s/16361b68674baa2e8949.

Author contributions

AR designed the study and completed GC-MS and GC-FID analyses. AM, CA, and CK completed XRD analyses. AS ran Raman analyses and DF ran EA-IRMS analyses. AP and HG assisted with experimental design and data interpretation. SJ supervised the study, and AR wrote the manuscript with assistance from all authors.

Acknowledgments

We are grateful for Jason P. Dworkin and Martin A. Carts at NASA GSFC for flame-sealing the tubes and irradiating the samples, as well as Angel Mojarro at the Massachusetts Institute of Technology (MIT) for assistance with GC-FID analyses. AR and SJ acknowledge support provided NASA award 80NSSC18K1140, and CA and CK acknowledge support provided by CRESST II CoOp award 80GSFC21M0002. DIF acknowledges funding provided by NASA awards 80NSSC20K0344, 80NSSC21K0654, 80NSSC21K0485, and 80NSSC19K0559.

Conflict of interest

The authors declare that the research was conducted in the absence of any commercial or financial relationships that could be construed as a potential conflict of interest.

Publisher's note

Supplementary material

The Supplementary Material for this article can be found online at: https://www.frontiersin.org/articles/10.3389/fspas.2022.919828/full#supplementary-material

References

Acuna, M. H., Connerney, J. E. P., Lin, R. P., Mitchell, D., Carlson, C. W., McFadden, J., et al. (1999). Global distribution of crustal magnetization discovered by the Mars Global Surveyor MAG/ER experiment. *Science* 284 (5415), 790–793. doi:10.1126/science.284.5415.790

Bristow, T. F., Grotzinger, J. P., Rampe, E. B., Cuadros, J., Chipera, S. J., Downs, G. W., et al. (2021). Brine-driven destruction of clay minerals in Gale crater, Mars. *Science* 373 (6551), 198–204. doi:10.1126/science.abg5449

Brocks, J. J., and Summons, R. E. (2003). "Sedimentary hydrocarbons, biomarkers for early life BT - treatise on geochemistry," in *Treatise on geochemistry* (Amsterdam, Netherlands: Elsevier), 63–115.

Dartnell, L. R., Desorgher, L., Ward, J. M., and Coates, A. J. (2007). Martian sub-surface ionising radiation: Biosignatures and geology. *Biogeosciences* 4 (4), 545–558. doi:10.5194/bg-4-545-2007

Dartnell, L. R. (2011). Ionizing radiation and life. *Astrobiology* 11 (6), 551–582. doi:10.1089/ast.2010.0528

Ehlmann, B. L., Mustard, J. F., Murchie, S. L., Bibring, J., Meunier, A., Fraeman, A. A., et al. (2011). Subsurface water and clay mineral formation during the early history of Mars. *Nature* 479, 53–60. doi:10.1038/nature10582

Eigenbrode, J. L. (2008). Fossil lipids for life-detection: A case study from the early Earth record. *Space Sci. Rev.* 135 (1–4), 161–185. doi:10.1007/s11214-007-9252-9

Eigenbrode, J. L., Summons, R. E., Steele, A., Freissinet, C., Millan, M., Navarro-González, R., et al. (2018). Organic matter preserved in 3-billion-year-old mudstones at Gale crater, Mars. *Science* 360, 1096–1101. doi:10.1126/science.aas9185

Ertem, G., Glavin, D. P., Volpe, R. P., and McKay, C. P. (2021). Evidence for the protection of N-heterocycles from gamma radiation by Mars analogue minerals. *Icarus* 368, 114540. doi:10.1016/j.icarus.2021.114540

Farley, K. A., Malespin, C., Mahaffy, P., Grotzinger, J. P., Vasconcelos, P. M., Milliken, R. E., et al. (2014). *In situ* radiometric and exposure age dating of the martian surface. *Science* 343, 1247166. doi:10.1126/science.1247166

Farley, Kenneth A., Williford, K. H., Stack, K. M., Bhartia, R., Chen, A., de la Torre, M., et al. (2020). Mars 2020 mission overview. *Space Sci. Rev.* 216 (8), 142. doi:10.1007/s11214-020-00762-y

Foustoukos, D. I., Alexander, C'O., and Cody, G. D. (2021). H and N systematics in thermally altered chondritic insoluble organic matter: An experimental study. *Geochimica Cosmochimica Acta* 300, 44–64. doi:10.1016/j.gca.2021.01.021

Fraeman, A. A., Ehlmann, B. L., Arvidson, R. E., Edwards, C. S., Grotzinger, J. P., Milliken, R. E., et al. (2016). The stratigraphy and evolution of lower Mount Sharp from spectral, morphological, and thermophysical orbital data sets. *J. Geophys. Res. Planets* 121, 1713–1736. doi:10.1002/2016je005095

Freissinet, C., Glavin, D. P., Mahaffy, P. R., Miller, K. E., Eigenbrode, J. L., Summons, R. E., et al. (2015). Organic molecules in the sheepbed mudstone, Gale crater, mars. *J. Geophys. Res. Planets* 120, 495–514. doi:10.1002/2014JE004737

Freissinet, C., Knudson, C. A., Graham, H. V., Lewis, J. M. T., Lasue, J., McAdam, A. C., et al. (2020). Benzoic acid as the preferred precursor for the chlorobenzene detected on mars: Insights from the unique cumberland analog investigation. *Planet. Sci. J.* 1, 41. doi:10.3847/PSJ/aba690

Glavin, D. P., Freissinet, C., Mahaffy, P. R., Miller, K. E., Eigenbrode, J. L., Summons, R., et al. (2015). "Martian chlorobenzene identified by curiosity in Yellowknife Bay: Evidence for the preservation of organics in a mudstone on mars," in 46th LPSC Lunar and Planetary Science Conference (Houston, TX: Lunar and Planetary Institute).

Grotzinger, J. P., Sumner, D. Y., Kah, L. C., Stack, K., Gupta, S., Edgar, L., et al. (2014). A habitable fluvio-lacustrine environment at Yellowknife Bay, Gale crater, mars. *Science* 343 (6169), 1242777. doi:10.1126/science.1242777

Horneck, G., and Baumstark-Khan, C. (2002). *Astrobiology: The quest for the conditions of life*. Berlin Heidelberg: Springer-Verlag.

Kminek, G., and Bada, J. L. (2006). The effect of ionizing radiation on the preservation of amino acids on Mars. *Earth Planet. Sci. Lett.* 245, 1–5. doi:10.1016/j.epsl.2006.03.008

Lüniger, G., and Schwark, L. (2002). Characterisation of sedimentary organic matter by bulk and molecular geochemical proxies: An example from oligocene maar-type Lake Enspel, Germany. *Sediment. Geol.* 148 (1–2), 275–288. doi:10.1016/S0037-0738(01)00222-6

Martin, P. E., Farley, K. A., Baker, M. B., Malespin, C. A., Schwenzer, S. P., Cohen, B. A., et al. (2017). A two-step K-Ar experiment on Mars: Dating the diagenetic formation of jarosite from Amazonian groundwaters. *J. Geophys. Res. Planets* 122, 2803–2818. doi:10.1002/2017JE005445

McMahon, S., Bosak, T., Grotzinger, J. P., Milliken, R. E., Summons, R. E., Daye, M., et al. (2018). A field guide to finding fossils on mars. *J. Geophys. Res. Planets* 123, 1012–1040. doi:10.1029/2017je005478

Mittelholz, A., Johnson, C. L., Feinberg, J. M., Langlais, B., and Phillips, R. J. (2020). Timing of the martian dynamo: New constraints for a core field 4.5 and 3.7 Ga ago. *Sci. Adv.* 6 (18), eaba0513. doi:10.1126/sciadv.aba0513

Moeller, R. C., Jandura, L., Rosette, K., Robinson, M., Samuels, J., Silverman, M., et al. (2021). The sampling and caching subsystem (SCS) for the scientific exploration of jezero crater by the mars 2020 perseverance rover. *Space Sci. Rev.* 217, 5. doi:10.1007/s11214-020-00783-7

Okon, A. (2010). "Mars science laboratory drill," in Proceedings of the 40th Aerospace Mechanisms Symposium. NASA/CP-20. Merritt, FL: NASA.

Pasteris, J. D., and Wopenka, B. (2003). Necessary, but not sufficient: Raman identification of disordered carbon as a signature of ancient life. *Astrobiology* 3, 727–738. doi:10.1089/153110703322736051

Pavlov, A. A., McLain, H. L., Glavin, D. P., Roussel, A., Dworkin, J. P., Elsila, J. E., et al. (2022). Rapid radiolytic degradation of amino acids in the Martian shallow subsurface: Implications for the search for extinct life. *Astrobiology* [Epub ahead of print]. doi:10.1089/ast.2021.0166

Pavlov, A. A., Vasilyev, G., Ostryakov, V. M., Pavlov, A. K., and Mahaffy, P. (2012). Degradation of the organic molecules in the shallow subsurface of Mars due to irradiation by cosmic rays. *Geophys. Res. Lett.* 39 (13), 5–9. doi:10.1029/2012GL052166

Peters, K. E., Clifford, W. C., and Moldowan, M. J. (2005). "The biomarker guide vol 1," in *Journal of chemical information and modeling* (Cambridge, United Kingdom: Cambridge University Press), 53, 9 1689–1699.

Poulet, F., Bibring, J.-P., Mustard, J. F., Gendrin, A., Mangold, N., Langevin, Y., et al. (2005). Phyllosilicates on Mars and implications for early Martian climate. *Nature* 438, 623–627. doi:10.1038/nature04274

Rampe, E. B., Blake, D., Bristow, T., Ming, D., Vaniman, D., Morris, R., et al. (2020). Mineralogy and geochemistry of sedimentary rocks and eolian sediments in Gale crater, mars: A review after six earth years of exploration with curiosity. *Geochemistry* 80 (2), 125605. doi:10.1016/j.chemer.2020.125605

Robinson, N., Eglinton, G., Cranwell, P. A., and Zeng, Y. B. (1989). Messel oil shale (Western Germany): Assessment of depositional palaeoenvironment from the content of biological marker compounds. *Chem. Geol.* 76 (1–2), 153–173. doi:10.1016/0009-2541(89)90134-4

Rojas Vivas, J. A., Navarro-Gonzáles, R., de la Rose, J., Molina, P., Sedov, S., McKay, C. P., et al. (2021). Radiolytic degradation of soil carbon from the mojave desert by 60 Co gamma rays: Implications for the survival of martian organic compounds due to cosmic radiation. *Astrobiology* 21, 381–393. doi:10.1089/ast.2020.2257

Simpson, J. A. (1983). Elemental and isotopic composition of the galactic cosmic rays. *Annu. Rev. Nucl. Part. Sci.* 33 (1), 323–382. doi:10.1146/annurev.ns.33.120183.001543

Squyres, S. W., and Kasting, J. F. (1994). Early mars: How warm and how wet? *Science* 265 (5173), 744–749. doi:10.1126/science.265.5173.744

Steele, A., Benning, L. G., Wirth, R., Schreiber, A., Araki, T., McCubbin, F. M., et al. (2022). Organic synthesis associated with serpentinization and carbonation on early Mars. *Science* 375, 172–177. doi:10.1126/science.abg7905

Steele, A., Benning, L. G., Wirth, R., Siljeström, S., Fries, M. D., Hauri, E., et al. (2018). Organic synthesis on Mars by electrochemical reduction of CO2. *Sci. Adv.* 4 (10), eaat5118. doi:10.1126/sciadv.aat5118

Steele, A., McCubbin, F. M., and Fries, M. D. (2016). The provenance, formation, and implications of reduced carbon phases in Martian meteorites. *Meteorit. Planet. Sci.* 51, 2203–2225. doi:10.1111/maps.12670

Steele, A., McCubbin, F. M., Fries, M. D., Golden, D. C., Ming, D. W., Benning, L. G., et al. (2012). Graphite in the martian meteorite allan hills 84001. *Am. Mineral.* 97, 1256–1259. doi:10.2138/am.2012.4148

Summons, R. E., Albrecht, P., McDonald, G., and Moldowan, J. M. (2008). Molecular biosignatures. *Space Sci. Rev.* 135 (1–4), 133–159. doi:10.1007/s11214-007-9256-5

Summons, R. E., Amend, J. P., Bish, D., Buick, R., Cody, G. D., Des Marais, D. J., et al. (2011). Preservation of martian organic and environmental records: Final report of the mars biosignature working group. *Astrobiology* 11 (2), 157–181. doi:10.1089/ast.2010.0506

Thorpe, M. T., Bristow, T. F., Rampe, E. B., Grotzinger, J. P., Fox, V. K., Bennett, K. A., et al. (2021). "The mineralogy and sedimentary history of the Glen Torridon region, Gale crater, Mars," in 52nd LPSC Lunar and Planetary Science Conference (The Woodlands, TX: Lunar and Planetary Institute).

Vago, J., Witasse, O., Svedhem, H., Baglioni, P., Haldemann, A., Gianfiglio, G., et al. (2015). ESA ExoMars program: The next step in exploring Mars. *Sol. Syst. Res.* 49 (7), 518–528. doi:10.1134/S0038094615070199

Vaniman, D. T., Bish, D. L., Ming, D. W., Bristow, T. F., Morris, R. V., Blake, D. F., et al. (2014). Mineralogy of a mudstone at Yellowknife Bay, Gale crater, mars. *Science* 343, 1243480. doi:10.1126/science.1243480